CERN-PH-TH/2013-251 24. 10. 13.

Causality Constraints on Hadron Production In High Energy Collisions

Paolo Castorina[a,b] **and Helmut Satz**[c]

a: Dipartimento di Fisica ed Astronomia, Universita' di Catania, Italy
b: PH Department, TH Unit, CERN, CH-1211 Geneva 23, Switzerland
c: Fakultät für Physik, Universität Bielefeld, Germany

Abstract

For hadron production in high energy collisions, causality requirements lead to the counterpart of the cosmological horizon problem: the production occurs in a number of causally disconnected regions of finite space-time size. As a result, globally conserved quantum numbers (charge, strangeness, baryon number) must be conserved locally in spatially restricted correlation clusters. This provides a theoretical basis for the observed suppression of strangeness production in elementary interactions (pp, e^+e^-). In contrast, the space-time superposition of many collisions in heavy ion interactions largely removes these causality constraints, resulting in an ideal hadronic resonance gas in full equilibrium.

1 Introduction

The temperature of the cosmic microwave background radiation (CBR) is, with a precision of up to one part in 10^5, found to be the same, some 2.7°Kelvin, throughout the observable universe. This constitutes one of the basic problems of Hot Big Bang cosmology, since at the end of the radiation era, when the CBR first appeared, the presently visible universe consisted of a huge number of causally disconnected spatial regions; for a schematic view, see Fig. 1. How could such a uniformity in temperature arise without any communication between the radiation sources?

The standard explanation has the equilibration arising either before or at inflation. In the inflation process, shortly after the Big Bang, the transition to the present stable vacuum ground state took place, accompanied by an exponential growth of the scale factor. This implies that when the present constituents of matter and radiation first appeared in our world, they were already in the same thermal state throughout all of space. They inherited this thermal behavior from a previous world of very much smaller dimension, in which they were in causal contact and hence able to equilibrate.

The evolution of elementary high energy collisions is generally described in terms of an inside-outside cascade [1]. It specifies a boost-invariant proper time τ_q, at which local volume elements experience the transition from an initial state of frozen virtual partons

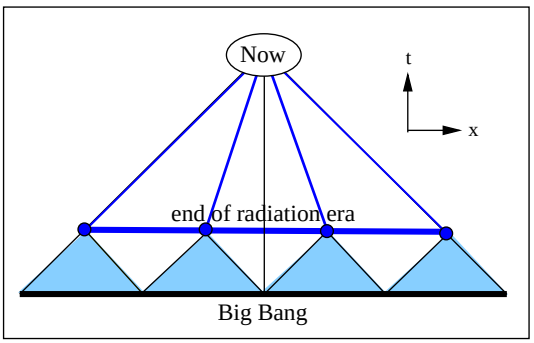

Figure 1: The origin of the observed cosmic background radiation

("color glass") to the on-shell partons which will eventually form hadrons. This partonisation time can be estimated most easily in e^+e^- annihilation (see Fig. 2).

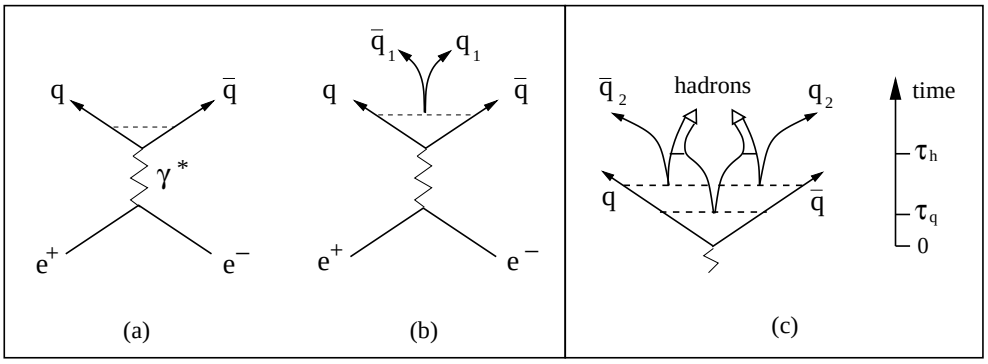

Figure 2: Initial stages of e^+e^- annihilation

The initial quark-antiquark pair is bound by a string of tension σ. When the separation distance x_q of the initial pair exceeds the energy $2\omega_q$ of an additional $q\bar{q}$ pair, the string breaks and the virtual pair is brought on-shell. For quarks of mass m_q, this energy is determined by

$$\sigma x_q = 2\sqrt{m_q^2 + k_T^2}, \tag{1}$$

where k_T is the transverse momentum of each quark in the newly formed pair. Through uncertainty relations, this is given by $k_T = \sqrt{\pi\sigma/2}$, leading to

$$x_q \simeq \sqrt{\frac{2\pi}{\sigma}} \simeq 1 \text{ fm}, \tag{2}$$

using $\sigma \simeq 0.2$ GeV^2 and $m_q \ll \sigma$. From this, we estimate

$$\tau_q \simeq \sqrt{\frac{\sigma}{2\pi}} \simeq 1 \text{ fm}. \tag{3}$$

This process is subsequently iterated, leading to a cascade of emitted $q\bar{q}$ pairs; while the first pair appears at rest in the center of mass of the annihilation process, the subsequent pairs are produced at increasing rapidities. The different pairs will eventually bind to

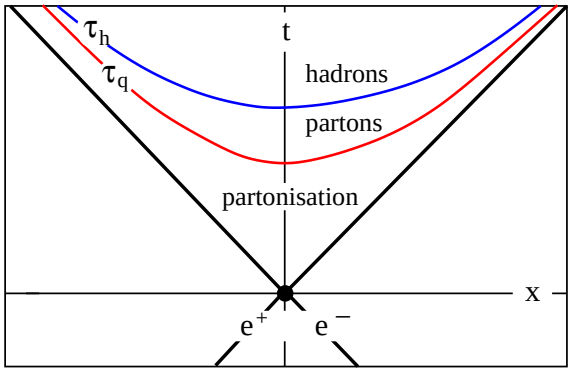

Figure 3: The evolution of e^+e^- annihilation

form free-streaming hadrons; for a boost-invariant evolution, this defines a second time threshold, the hadronisation time $\tau_h > \tau_q$. The overall scheme is summarized in Fig. 3.

The generalization to pp collisions is straight-forward: again there is a finite time τ_q needed to bring the partons on-shell, and after a larger time τ_h, these combine to form hadrons. We denote the bubbles of medium for proper time τ, with $\tau_q < \tau < \tau_h$, as "fireballs". Hadronisation thus occurs through the formation of partonic fireballs in a cascade of increasing rapidities. In a boost-invariant scheme, the center of mass space-time coordinates x, t, with x denoting the collision axis, are related to proper time τ and spatial rapidity η through

$$t = \tau \cosh \eta, \quad x = \tau \sinh \eta, \tag{4}$$

with $c = 1$. The resulting evolution is illustrated in Fig. 4, where the transition curves are determined by $t^2 - x^2 = \tau^2$. Schematically included in this figure is a fireball at $\eta = 0$ and one at a larger η.

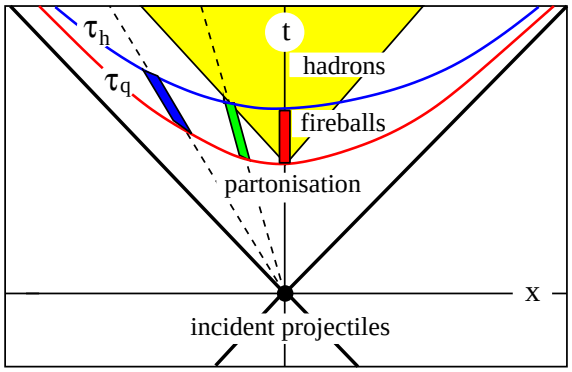

Figure 4: The boost-invariant evolution of a high energy collision, from the partonisation stage ($\tau \leq \tau_q$) to a fireball ($\tau_q \leq \tau \leq \tau_h$) to hadrons ($\tau \geq \tau_h$). The region causally connected to a fireball at $\eta = 0$ is colored in yellow, the fireball itself in red. An identical fireball for $\eta = \eta_d$ is marked in green, one for $\eta > \eta_d$ in blue.

Both the partonisation and the hadronisation points for the system at larger η are seen to be well outside the future region of the $\eta = 0$ fireball. More specifically, the hadronization

point for the large η fireball just touches the event horizon of the $\eta = 0$ fireball for

$$\tanh \eta_d = \frac{\tau_h^2 - \tau_q^2}{\tau_h^2 + \tau_q^2}, \tag{5}$$

defining the fireball range causally connected to the system at $\eta = 0$. Beyond this rapiditiy, i.e., for $\eta > \eta_d$, the two fireballs are causally disconnected and cannot synchronize each other's thermal status. For the moment we are here neglecting the spatial extension of the fireball, but we shall return to this aspect shortly.

To illustrate, we choose $\tau_q = 1$ fm and $\tau_h = 2$ fm; in this case, a fireball with $\eta > 0.7$ cannot communicate with one at $\eta = 0$. The longer the fireball lifetime is, the larger is the rapidity range of fireballs in causal communication with that at $\eta = 0$. The increase of the range with fireball lifetime is quite slow, however; even for $\tau_h = 7$ fm, the rapidity horizon is only $\eta_d = 2$. In other words, collisions at RHIC or at the LHC will lead to hadron production from causally disconnected fireballs.

The observation just made does not, of course, rule out a causal connection (and hence correlations) for hadron production at large rapidity intervals; it only means that any correlations must have originated in the earlier partonisation stage. It does imply, however, that any state formed at $\eta = 0$ after a finite time interval cannot synchronize its thermal status with a corresponding state at larger rapidity. We thus conclude that the fireballs formed in elementary high energy collisions appear in causally disconnected regions, which cannot communicate and thus in particular cannot establish a uniform temperature. If the hadronization temperature is found to be the same for different kinematic regions, this must be due to the local hadronization nature. There does not exist some large equivalent global system in thermal equilibrium, since any such equilibrium requires communication.

2 Causal Connection of Fireballs

In the previous section, we had obtained in eq. 5 the maximum rapidity η_d for which a fireball could still receive a signal from a one at $\eta = 0$. Here the spatial extension of the fireball was for simplicity neglected. For a more realistic situation, we have to consider a fireball of finite spatial extent. We take the longitudinal extension of the system to be vanishingly small at the interaction time $t = 0$; for sufficiently high energy, this is expected to be a good approximation. The evolution of the system is shown in Fig. 5, where the shaded area defines the fireball produced at rest in the CMS. The extremal velocity lines $\pm\beta = \pm v/c$ specify the spatial size of this fireball at the time τ_q of formation and its expansion up to the hadronisation time τ_h. To consider the system as one fireball, we require that the spatially right-most point q_R at formation can send a signal to the spatially left-most point h_L at hadronisation; i.e., we require that the most separate points of the fireball can still communicate. This definition of a "causal" fireball is evidently an upper limit in size; one may wish to impose more stringent conditions and obtain a smaller fireball. We will keep that in mind in what follows. The crucial requirement in our case is that the world-line connecting q_R on the τ_q hyperbola with the point h_L on the τ_h hyperbola is light-like, as shown in Fig. 5.

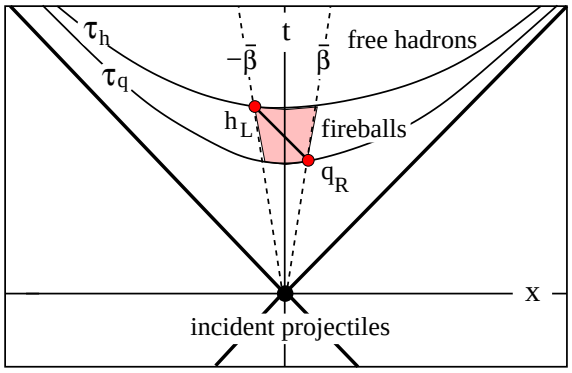

Figure 5: The formation and evolution of a fireball at rest in the center of mass; the fireball evolution is indicated in pink.

To determine the resulting value of the velocity β, we note that the point q_R has the coordinates

$$q_R = \left[\frac{\tau_q}{\sqrt{1-\beta^2}}, \frac{\beta\tau_q}{\sqrt{1-\beta^2}}\right], \tag{6}$$

while h_L is given by

$$h_L = \left[\frac{\tau_h}{\sqrt{1-\beta^2}}, -\frac{\beta\tau_h}{\sqrt{1-\beta^2}}\right]. \tag{7}$$

The light ray eminating from q_R is described by

$$-\left(t - \frac{\tau_q}{\sqrt{1-\beta^2}}\right) = x - \frac{\beta\tau_q}{\sqrt{1-\beta^2}}. \tag{8}$$

Imposing that h_L lies on this line leads to

$$\beta = \frac{\tau_h - \tau_q}{\tau_h + \tau_q} \tag{9}$$

and thus determines the rapidity with which the edges of the central fireball move out by its expansion. The resulting spatial extension of this fireball becomes

$$d = \frac{2\beta\tau_h}{\sqrt{1-\beta^2}} = \sqrt{\frac{\tau_h}{\tau_q}}(\tau_h - \tau_q), \tag{10}$$

measured at the time of hadronisation in the center of mass and thus in the proper frame of the fireball. This is the maximum initial size the fireball can have and still retain in its life-time a causal connection between its most distant space-time points. It is therefore fully determined by the proper fireball formation time τ_q and its proper life-time $\tau_h - \tau_q$. In table 1, we show the resulting velocities β and rapidities η for the fireball edges and the radii ($r = d/2$) of the fireballs produced at rest in the center of mass at $\tau_q = 1$ fm, for different values of the fireball life-time. Of course the size of the fireball increases with increasing hadronisation time; it is only the finite life-time of the partonic state that causes the total rapidity range for production to become divided into causally disconnected segments. The rapidity extension of a fireball, as we have defined it here, is

τ_h [fm]	β	η	r [fm]
2	0.33	0.35	0.7
3	0.50	0.55	1.7
4	0.60	0.69	3.0
5	0.67	0.81	4.5

Table 1: Velocity (β) and rapidity (η) limits of a fireball at rest in the center of mass, and its proper hadronisatin radius r, as given by eqs. 9 and 10, for a formation time $\tau_q = 1$ fm and different hadronisation times τ_h.

roughly plus/minus one unit for $\tau_q = 1$ fm, $\tau_h = 3$ fm; its (proper) spatial radius at the time of formation is about 2 fm.

We now assume complete boost invariance: the collision leads to the production of identical fireballs at all rapidities, with identical formation and hadronisation times τ_q, τ_h in their respective rest frames. To study the causal connection of fireballs moving at different rapidities, it is helpful to introduce a more specific notation for their velocities. We denote the velocity of the fireball at rest in the CMS by $\bar{\beta}_0 = 0$, and its extremal velocities by $\beta_{0L} = -\beta$ and $\beta_{0R} = \beta$. The neighboring fireball then has a central velocity $\bar{\beta}_1$ and extremal velocities β_{1L} and β_{1R}. In its own rest-frame, this fireball will have the same evolution pattern and spatial size as the one at rest in the center of mass. To define a causal connection between this fireball and the one at rest in the center of mass, we determine the largest value of $\bar{\beta}_1$, which still allows any point of the moving fireball to receive at (the latest) time τ_h a signal from at least one point of the CMS fireball emitted at (the earliest) time τ_q, and vice versa, for the cms fireball. The relevant geometry is illustrated in Fig. 6. It is evident that the left extreme world-line of the central fireball must then coincide with the right extreme of the fireball moving with velocity $-\bar{\beta}_1$. In other words, two adjacent fireballs of identical structure will, in the sense just defined, be causally connected. The next one "down the line", however, with velocity $\bar{\beta}_2$, is causally disconnected from the central fireball.
The determination of the central velocities of the successive fireballs is given in the appendix; the result is

$$\beta_n = \frac{\tau_h^{2n} - \tau_q^{2n}}{\tau_h^{2n} + \tau_q^{2n}}, \quad n = 0, 1, 2, ... \tag{11}$$

Similarly, we obtain for the left extremal velocity of the n-th fireball

$$\beta_{nL} = \frac{\tau_h^{2n+1} - \tau_q^{2n+1}}{\tau_h^{2n+1} + \tau_q^{2n+1}}, \quad n = 0, 1, 2, ..., \tag{12}$$

where β_{0L} reduces to the value already given by eq. 9 for the fireball at rest in the overall center of mass. Moreover, quite generally $\beta_{nL} = \beta_{(n+1)R}$. We have thus divided the thermal space-time region, between τ_q and τ_h, into separate (non-overlapping) fireballs, such that next neighbors are causally connected, all further ones not.

To illustrate the mesh of the net thus obtained, we list in table 2 the values of the velocities and rapidities of the first moving fireball, as measured in the CMS, for the fireball life-

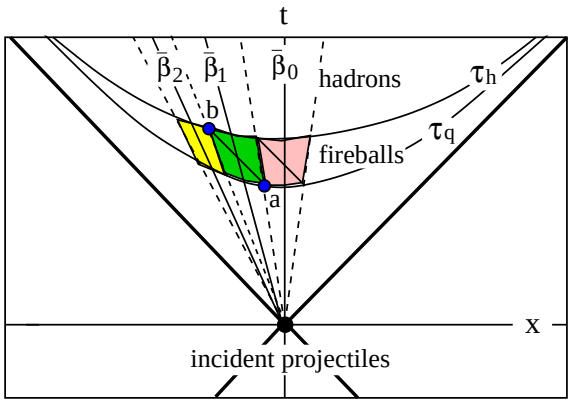

Figure 6: The formation and evolution of two fireballs, one at rest in the center of mass (pink), one moving with velocity $\bar{\beta}_1$ (green). The light line from a to b determines the largest velocity difference still allowing a full causal connection between the two fireballs. For illustration, a third (yellow) fireball is shown, moving with velocity $\bar{\beta}_2$ and not causally connected to the one at rest in the center of mass.

τ_h [fm]	β_1	η_1
2	0.60	0.70
3	0.80	1.10
4	0.88	1.39
5	0.92	1.61

Table 2: Limiting velocities and rapidities for a moving fireball to have causal connection with one at rest in the center of mass, see eq.(9)

times used above. These values specify the maximum rapidity a moving fireball can have and still remain causally connected to the one at rest in the CMS.

3 Hadronisation of Fireballs

The hadrons formed through the final parton fusion constitute in principle a complex interacting medium. A great simplification of this situation is provided by an old argument [2, 3]: if the interactions between the basic hadrons, mesons and baryons, are resonance-dominated, then the interacting system of ground state hadrons can be replaced by an ideal gas of all possible resonances. The relative abundances of the different hadrons are in this case determined simply by the corresponding phase space weights, specified in terms of the hadron masses and intrinsic degrees of freedom.

The resulting statistical hadronisation model, based on a ideal gas of all observed hadronic resonances, provides an excellent general account for hadron production in high energy collisions, from e^+e^- annihilation to the collision of heavy nuclei (see, e.g., [4–7], and further references given there). All high energy data lead to a universal hadronisation temperature around 160 MeV, in accord with the pseudo-critical temperature found in finite temperature lattice QCD with physical quark masses and for vanishing or low baryon

density. This raises the question if and how hadronisation in elementary collisions differs from that in nucleus-nucleus interactions. Here the crucial observation is that in elementary collisions, the production of hadrons containing n strange quarks or antiquarks is reduced in comparison to the ideal resonance gas prediction. This reduction can be accounted for by the introduction of a universal strangeness suppression factor γ_s^n, where n denotes the number of strange quarks and/or antiquarks contained in the hadron in question [8]. The value of γ_s is rather energy-independent and found to be around 0.5 to 0.7, from some 20 GeV up to LHC energies. In nuclear collisions, in contrast, γ_s appears to converge to unity at RHIC and LHC energies, apart from slight corrections presumably due to corona effects [9, 10].

The statistical hadronization model assumes that hadronization in high energy collisions is a universal process proceeding through the formation of multiple massive colorless clusters or fireballs of finite spacial extension and distributed over the rapidity range of the process. These clusters are taken to decay into hadrons according to a purely statistical law: every multi-hadron state of the cluster phase space defined by its mass, volume and charges is equally probable. The mass distribution and the distribution of charges (electric, baryonic and strange) among the clusters and their (fluctuating) number are determined in the prior dynamical stage of the process. Hence in principle one would need the mentioned dynamical distributions in order to make definite quantitative predictions. However, for Lorentz-invariant quantities such as multiplicities, one can further simplify matters by assuming that the distribution of masses and charges among clusters is again purely statistical, so that, as far as the calculation of multiplicities is concerned, the set of clusters becomes equivalent, on average, to one large cluster, the *equivalent global cluster*, whose volume is the sum of proper cluster volumes and whose charge is the sum of cluster charges, and thus the conserved charge of the initial colliding system. In such a global averaging process, the equivalent cluster in many cases turns out to be large enough in mass and volume so that the canonical ensemble becomes a good approximation.

To obtain a simple expression for our further discussion, we neglect for the moment an aspect which is important in any actual analysis. Although in elementary collisions the conservation of the various discrete Abelian charges (electric charge, baryon number, strangeness, heavy flavour) has to be taken into account *exactly* [12], we here consider for the moment a grand-canonical picture. We also assume Boltzmann distributions for all hadrons. The multiplicity of a given scalar hadronic species j then becomes

$$\langle n_j \rangle^{\text{primary}} = \frac{VTm_j^2}{2\pi^2} \gamma_s^{n_j} \mathrm{K}_2\left(\frac{m_j}{T}\right) \tag{13}$$

with m_j denoting its mass and n_s the number of strange quarks/antiquarks it contains. Here primary indicates that it gives the number at the hadronisation point, prior to all subsequent resonance decay. The Hankel function $K_2(x)$, with $K(x) \sim \exp\{-x\}$ for large x, gives the Boltzmann factor, while V denotes the overall equivalent cluster volume. In other words, in an analysis of 4π data of elementary collisions, V is the sum of the all cluster volumes at all different rapidities. It thus scales with the overall multiplicity and hence increases with collision energy. A fit of production data based on the statistical hadronisation model thus involves three parameters: the hadronisation temperature T, the strangeness suppression factor γ_s, and the equivalent global cluster volume V.

We want to use the results of the present paper to show that the nature of V in elementary collisions is quite different from that in nuclear collisions, and this can in effect lead to different behavior in the two cases. Strangeness production is perhaps the most readily accessible such phenomenon. In elementary collisions, the clusters at rapidities sufficiently far apart are, as we have seen, causally disconnected, so that they cannot exchange information. Hence strangeness must be conserved locally; in *pp* collisions, for example, each cluster must have strangeness zero. Thus typically there will be only one pair of strange particles within a given cluster, adding up to zero total cluster strangeness. Such a local strangeness conservation is known to lead to a suppression of strangeness production [11]; we return to details shortly. In high energy nuclear collisions, on the other hand, the equivalent global cluster consists of the different clusters from the different nucleon-nucleon interactions at a common rapidity. At mid-rapditiy, for example, we thus have the sum of the superimposed mid-rapidity clusters from the different nucleon-nucleon collisions, and these are all causally connected, allowing strangeness exchange and conservation between the different clusters.

As noted, the local conservation of charges, and in particular of strangeness, has in fact been proposed for quite some time as the mechanism responsible for strangeness suppression [11]; more details are given in appendix A2. In the grand canonical approach, the introduction of the suppression factor γ_s achieves the observed suppression. The alternative of local strangeness suppression is based on two features. First, one imposes exact strangeness conservation, which leads to a volume-dependent strangeness reduction [12, 13]; the ratio of canonical to grand-canonical partition functions,

$$\frac{Z_{\rm can}(T,V,S)}{Z_{\rm gcan}(T,V,\langle S\rangle)} < 1 \tag{14}$$

approaches unity only in the limit of large volumes. However, in elementary collisions with the corresponding overall equivalent cluster volume, the resulting reduction is not sufficient to account for the observed strange particle rates. Hence it was argued that if in a given collision only one pair of strange hadrons is produced, these should appear close to each other spatially, the more so if the medium is relatively short-lived. This approach thus introduces somewhat *ad hoc* a strangeness correlation volume $V_c < V$, within which strangeness has to be conserved exactly. The corresponding model thus now has T, V and V_c as the parameters to be specified by the data, and fits based on such a model provide as good an account for the data as the earlier γ_s scheme [14, 15], with the exception of the ϕ, to which we return later. However, *a priori* little is known about V_c, and in particular it remains open what happens to it in nuclear collisions.

We here propose that the strangeness correlation volume V_c is in fact that of a causally connected cluster; causal connectivity thus provides the fundamental reason for local strangeness conservation and hence for the strangeness suppression observed in elementary interactions. It is moreover clear that in nucleus-nucleus interactions, the overlapping fireballs produced at fixed rapidity by the different nucleon-nucleon collisions will give rise to a much larger causally connected volume and thus effectively remove the locality constraints. Moreover, if *very* high energy *pp* interactions lead to multiple jet production, this could eventually lead to a similar effect, with overlapping clusters from the different jet directions.

We have seen how the size of the causally connected cluster volumes varies with the fireball life-time. An obvious question therefore is whether the fits to production data lead to reasonable cluster sizes. It is found [14, 15] that good fits to data at $\sqrt{s} = 17.3$ and 200 GeV require a strangeness correlation radius of about 1 fm, while leading to the same universal hadronisation temperature of about 160 MeV. In our considerations, this is seen to be in accord with a hadronisation time τ_h of about 2 - 3 fm. For an evolution of the kind shown in Fig. 2 that makes good sense: it takes about 1 fm to form the first $q\bar{q}$ pair, and another to have it hadronize. The causality constraints in elementary high energy collisions thus appear to provide the reason for the observed strangeness suppression, thereby justifying the strangeness correlation model [11].

We further note here that in elementary collisions, hadronisation as Unruh radiation arising from quarks tunnelling through their color confinement horizon [16] inherently contains locals strangeness conservation. In such a scheme, the maximum separation between s and $\bar{s}$ can never exceed the hadronic scale leading to string breaking, i.e., about 1 fm, thus enforcing strangeness production in a very restricted spatial volume.

In the case of heavy nuclei, on the other hand, we find in the center of mass with increasing collision energy a superposition of more and more individual nucleon-nucleon interactions in the same space-time region. At high enough collision energy, there will thus be on the average around five or six superimposed nucleon-nucleon collisions, so that there now exists a causally connected region having an effective volume five or six times larger than that in a nucleon-nucleon collision, with a corresponding increase in the number of produced strange particles. An s quark produced in any specific nucleon-nucleon collision now finds so many $\bar{s}$ from other such collisions in its immediated environment that no spatial constraints on its partner $\bar{s}$ are necessary. Moreover, the superposition of collisions at central rapidity greatly increases the partonic density there. As a consequence, it takes a longer time for the system to expand up to the hadronisation point, so that τ_h now is considerably larger. This aspect further increases the correlation volume. In terms of a conventional statistical description, it implies that γ_s is driven towards unity. At $\sqrt{s} = 17.3$ GeV, the overlap is not yet complete: when the first nucleons collide, those at the opposite edges of the two nuclei are still some 3 fm apart, so that we can still expect some strangeness suppression, and this is indeed observed. At $\sqrt{s} = 200$ GeV, this separation has decreased to 0.3 fm, so that at RHIC and at the LHC, there should not be any suppression, apart from possible corona contributions.

4 The Problem of Hidden Strangeness

The approach presented here for the suppression of strangeness production in elementary collisions contains one open issue, which arises in all attempts of local strangeness conservation. It is found experimentally that the ϕ meson, consisting of an $s\bar{s}$ pair, is also suppressed, although from a hadronic point of view, it is of zero strangeness. In the conventional statistical model with a strangeness suppression factor, the power of γ_s is determined by the number of s plus $\bar{s}$ quarks a given hadron contains. Hence the ϕ gets a factor γ_s^2, which leads to rough agreement with the data. In contrast, in a canonical formulation on a hadronic level, the ϕ does not present any quantum number to be conserved exactly and is not subject to any suppression. There are (at least) two ways to

resolve this issue.

It is well-known that quarkonia ($c\bar{c}$ and $b\bar{b}$ mesons, states of hidden heavy flavor) cannot be accommodated at all in any statistical approach. Their production and binding is governed by gluon dynamics instead. One might therefore argue that the ϕ, as hidden strangeness meson, also falls into this category and hence its abundance cannot be determined in a statistical model. However, such an approach has its own problems. The abundance of charmonium and bottomonium states is *underpredicted* by orders of magnitude, while that of the ϕ is *overpredicted* by a factor four or so. The quarkonium states are below the open charm/beauty thresholds, while the ϕ decays strongly into a $K\bar{K}$ pair. Finding a common ground for it and the quarkonia is therefore surely not easy.

Another approach is that taken in the introduction of the suppression factor γ_s in powers of the content of strange *and* antistrange quarks. The evolution of the statistical hadronisation went from grand-canonical to canonical, and on to the introduction of a correlation volume in the hadronic canonical formulation. The disagreement of the ϕ abundance may thus be nature's way of telling us that strangeness correlation really occurs already on a pre-hadronic level. Requiring exact strangeness conservation for the quark system in the fireball prior to hadronisation would in fact result in canonical strangeness suppression of both open and hidden strangeness (see Fig. 7), of a functional form very similar to that obtained on a hadronic level in Appendix 2.

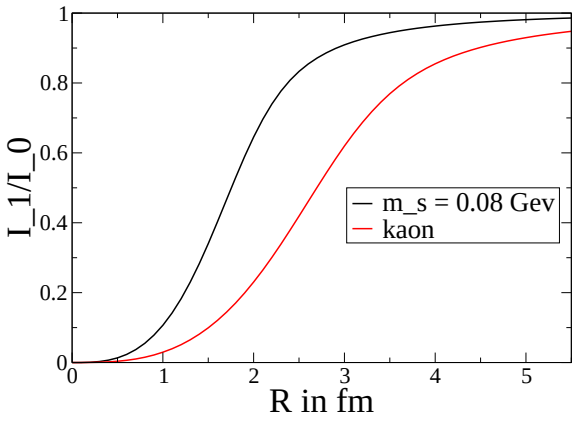

Figure 7: The suppression factor for exact strangeness conservation of strange quarks of mass $m_s = 80$ MeV in a volume of radius R, compared to the suppression factor of kaons (see appendix 2), both at a temperature of 160 MeV.

Acknowledgements The authors thank F.Becattini and U.Wiedemann for stimulating discussions. P.C. thanks the CERN TH-unit for the hospitality.

References

[1] J. D. Bjorken, Lecture Notes in Physics (Springer) 56 (1976) 93.

[2] E. Beth and G. E. Uhlenbeck, Physica 4 (1937) 915.

[3] R. Dashen, S.-K. Ma and H. J. Bernstein, Phys. Rev. 187 (1969) 345.

[4] F. Becattini and G. Passaleva, Europ. Phys. J. C23 (2002) 551.

[5] P. Braun-Munzinger, K. Redlich and J. Stachel, in *Quark-Gluon Plasma 3*, R. C. Hwa and X.-N Wang (Eds.), World Scientific, Singapore 2003.

[6] F. Becattini and R. Fries, arXiv:0907.1031 [nucl-th], and Landolt-Boernstein 1-23.

[7] F. Becattini et al., Europ. Phys. J. CC 66 (2010) 377.

[8] J. Letessier, J. Rafelski and A. Tounsi, Phys. Rev. C64 (1994) 406.

[9] F.Becattini and J.Manninen Phys. Lett. B 673 (2009) 19.

[10] J. Aichelin and K. Werner, Phys. Rev. C 79 (2009) 064907.

[11] J. S. Hamieh, K. Redlich and A. Tounsi, Phys. Lett. B 486 (2000) 61.

[12] R. Hagedorn and K. Redlich, Z. Phys. C27 (1985) 541

[13] for further details, see e.g., P. Braun-Munzinger, K. Redlich and J. Stachel in *Quark-Gluon Plasma 3*, R. C. Hwa and X.-N. Wang (Eds.), World Scientific, Singapore 2003.

[14] I. Kraus et al., Phys. Rev. C76 (2007) 064903.

[15] I. Kraus et al., Phys. Rev. C79 (2009) 014901.

[16] P. Castorina, D. Kharzeev and H. Satz, Europ. Phys. J. C52 (2007) 187.

Appendix A1

According to the criterium of causal connection discussed in Section 2, the world-lines of the left extremum and of the right extremum of the fireball n, with $n \geq 1$, in the region $x < 0$ are, respectively, $-\beta_{n+1}t = x$ and $-\beta_n t = x$ (see Fig. 6).

The right extremum meets the hyperbola of the plasma formation time, $t^2 - x^2 = \tau_q^2$, at the event point E_a with coordinates

$$(t_n^q, x_n^q) = (\frac{\tau_q}{\sqrt{1-\beta_n^2}}, \frac{-\beta_n \tau_q}{\sqrt{1-\beta_n^2}}). \tag{15}$$

The light ray originating from the point E_a has equation

$$-t + \frac{\tau_q}{\sqrt{1-\beta_n^2}} = x - \frac{\beta_n \tau_q}{\sqrt{1-\beta_n^2}} \tag{16}$$

and crosses the hyperbola of the hadronization time, $t^2 - x^2 = \tau_h^2$, at the event point E_b with coordinates

$$(t^h, x^h) = \left(\frac{1}{2\tau_q} \sqrt{\frac{1+\beta_n}{1-\beta_n}} \left[\tau_h^2 + \tau_q^2 \frac{1-\beta_n}{1+\beta_n} \right], \frac{1}{2\tau_q} \sqrt{\frac{1+\beta_n}{1-\beta_n}} \left[\tau_h^2 - \tau_q^2 \frac{1-\beta_n}{1+\beta_n} \right] \right). \tag{17}$$

Since the event E_b has to be on the world line of the left extremum, we must have $\beta_{n+1} = -x^h/t^h$, i.e.

$$\beta_{n+1} = \left(\tau_h^2 - \tau_q^2 \frac{1-\beta_n}{1+\beta_n} \right) \Big/ \left(\tau_h^2 + \tau_q^2 \frac{1-\beta_n}{1+\beta_n} \right), \tag{18}$$

expressing our condition of causal connection. The first extremal world-line in the $x < 0$ region has speed (see eq.(9))

$$\beta_1 = \frac{\tau_h - \tau_q}{\tau_h + \tau_q}, ; \tag{19}$$

hence $(1-\beta_1)/(1+\beta_1) = \tau_q/\tau_h$, and, by iteraction, the speeds of the left extrema are found to be ($n \geq 0$)

$$\beta_{n+1} = \frac{\tau_h^{2n+1} - \tau_q^{2n+1}}{\tau_h^{2n+1} + \tau_q^{2m+1}} \tag{20}$$

The speed of the cms of the n-th fireball, $\bar{\beta}_n$, with respect to the rest frame (corresponding to the cms of the fireball at $x = 0$) is defined by requiring that all fireballs have the same structure in their cms. In other words, if β_{n+1} and β_n are the speeds of the two extrema of a fireball n in the overall rest frame, and β'_{n+1} and β'_n are the corresponding velocities in the rest frame of this fireball, the speed $\bar{\beta}_n$ of the cms of the fireball with respect to the overall rest frame must be such that $\beta'_{n+1} = -\beta'_n$. By the velocity composition law, it turns out that

$$\bar{\beta}_n = \frac{(1 + \beta_{n+1}\beta_n) - \sqrt{(1-\beta_{n+1}^2)(1-\beta_n^2)}}{\beta_{n+1} + \beta_n} \tag{21}$$

By eq. (18) and after some algebra, one obtains

$$\bar{\beta}_n = \frac{\left[\tau_h(1+\beta_n) - \tau_q(1-\beta_n)\right]^2}{\tau_h^2(1+\beta_n)^2 - \tau_q^2(1-\beta_n)^2}. \tag{22}$$

By use of eq. (19) and some iteration, this gives

$$\bar{\beta}_n = \frac{\tau_h^{2n} - \tau_q^{2n}}{\tau_h^{2n} + \tau_q^{2n}}. \tag{23}$$

for the speed of fireball n.

Appendix A2

We here want to illustrate in some detail the mechanism of local strangeness reduction. To simplify matters, let us assume that there are only two hadron species: scalar and electrically neutral mesons, "pions" of mass m_π, "kaons" of mass m_K and strangeness

$s = 1$ together with "antikaons" of the same mass but strangeness $s = -1$. In this case, the grand canonical partition function for a system of of volume V and temperature T has the form

$$Z_{GC}(T, V, \mu) = \frac{VT}{2\pi^2}\left[m_\pi^2 K_2(m_\pi/T) + m_K^2 K_2(m_K/T)e^{\mu/T} + m_K^2 K_2(m_K/T)e^{-\mu/T}\right], \quad (24)$$

where μ denotes the chemical potential for strangeness. If the overall strangeness is zero, $\mu = 0$ and the average density of mesons of type i ($i = \pi, K, \bar{K}$) is given by

$$n_i(T) = \frac{Tm_i^2}{2\pi^2} K_2(m_i/T), \quad (25)$$

while the ratio of kaon to pion multiplicities becomes

$$\frac{N_K}{N_\pi} = \left(\frac{m_K}{m_\pi}\right)^2 \frac{K_2(m_K/T)}{K_2(m_\pi/T)} \simeq \left(\frac{m_K}{m_\pi}\right)^{3/2} \exp\{-\frac{(m_K - m_\pi)}{T}\}. \quad (26)$$

Both species densities and ratios thus are independent of the overall volume V; they are determined by the respective masses and the hadronisation temperature T. The grand canonical form assures that the average overall strangeness is zero, but only the *average*; there are fluctuations, and, for example, the second cumulant

$$\left(\frac{\partial^2 \ln\, Z_{GC}}{\partial \mu^2}\right) \sim \langle S^2 \rangle \quad (27)$$

indicates that the average of the squared strangeness does not vanish.

The grand canonical ensemble effectively corresponds to an average over all possible strangeness configurations, with $\exp(\pm\mu/T)$ as weights. If instead we insist that the overall strangeness is *exactly* zero, we have to project out that term of the sum. This canonical ensemble can lead to a severe restriction of the available phase space and hence of the production rate. Thus the canonical density of kaons becomes [11, 13]

$$\tilde{n}_K(T, V) = n_K(T)\frac{I_1(x_K)}{I_0(x_K)}, \quad (28)$$

where $I_n(X)$ is the $n-th$ order Bessel function of imaginary argument and $n_K(T)$ is given by eq. (25) and

$$x_K = \frac{VTm_K^2}{2\pi^2} K_2(m_K/T). \quad (29)$$

The canonical density, in contrast to the grand canonical form, thus depends on the volume V of the system. Since $I_n(x) \sim x^n$ for $x \to 0$ and $I_n(x) \to e^x$ for $x \to \infty$, we see immediately that in the large volume limit,

$$\tilde{n}_K(T, V) \to n_K(T), \quad (30)$$

the canonical form converges to the grand canonical one, as expected. In the small volume limit, however, the Bessel function ratio results in a strong suppression of canonical relative to grand canonical form, with $I_1(x)/I_0(x) \to 0$ for $x \to 0$. For the actual values of the

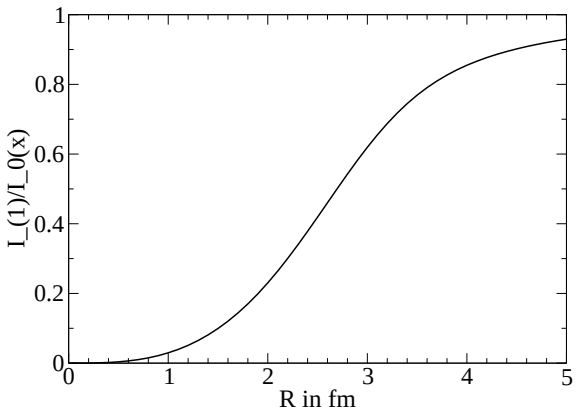

Figure 8: The suppression factor for exact strangeness conservation of kaons in a volume of radius R.

kaon mass and $T \simeq 160$ MeV, this suppression sets in for volumes of radii less than some 2 - 3 fm; above that, the grand canonical form becomes valid. The form of the suppression factor is shown in Fig. 8; we recall that strange baryons are neglected in obtaininng eq. 28, so that the figure is for illustration only.

We thus see that the exact conservation of charges, such as strangeness, results in a "canonical suppression" for sufficiently small volumes. Now the overall volume V in the conventional description of e^+e^- annihilation or in pp collisions is that of the equivalent cluster and hence determined largely by the number of pions. Thus imposing exact strangeness conservation here is not the solution - the total volume is so large that there is no effective canonical suppression. To obtain the observed strangeness reduction, an additional mechanism is necessary.

This was obtained [11] by arguing that in the case of very few charge carriers, charge neutralisation must occur in a correlation volume V_c very much smaller than the overall volume V. For a given charge, there must be an opposite charge nearby, not some large distance away. This argument was supported by kinetic studies, indicating that the typical life-time of the partonic medium is not sufficient for far-away charges to meet, making exact conservation unlikely. As a result, the partition function for our pion-kaon system now becomes for exact strangeness zero

$$Z(T,V,V_c) = \frac{VT}{2\pi^2}\left[m_\pi^2 K_2(m_\pi/T) + 2m_K^2 K_2(m_K/T)\left(\frac{I_1(x_K(T,m_K,V_c))}{I_0(x_K(T,m_K,V_c))}\right)\right], \qquad (31)$$

where the argument of the Bessel functions is given by

$$x_K = \frac{V_c T m_K^2}{2\pi^2} K_2(m_K/T). \qquad (32)$$

and thus contains the strangeness correlation volume V_c as further parameter. By tuning V_c, we can thus achieve as much strangeness suppression as desired.

As mentioned, our considerations here are only meant as illustration. In actual studies, both normal, strange and multi-strange baryons have to be included, as well as all higher resonant states. If this is done, a formulation of the type discussed here leads with a

correlation radius R_c around 1 fm to the observed suppression and to a model which can account for the data from elementary collisions as well as the conventional γ_s approach, except for the mentioned ϕ problem.